DOI 10.1515/freq-2012-0137 — Frequenz 2013; 67(7–8): 213–221

J. Valarmathi*, D. S. Emmanuel and S. Christopher

# Interpolated Adaptive Doppler Filter for Estimating Velocity

**Abstract:** This paper discusses the application of Lagrange interpolation and cubic spline interpolation to predict acceleration/velocity and to adapt better window lengths for any range of target acceleration. The estimated velocity/acceleration is then smoothed using Kalman and adaptive Kalman filters. Simulation results show that in a 'high-level noise' scenario, the interpolated adaptive filter gives a more accurate estimation than the existing method of using a rectangular window function. Track initialization error minimized with spline interpolation was comparable to that minimized with Lagrange interpolation.

**Keywords:** Lagrange's polynomial, cubic spline, Kalman filter, adaptive Kalman filter

***Corresponding author: J. Valarmathi:** School of Electronics Engineering, VIT University, Vellore 632014, India
E-mail: jvalarmathi@vit.ac.in
**D. S. Emmanuel:** School of Electronics Engineering, VIT University, Vellore 632014, India
**S. Christopher:** Centre for Airborne System, Ministry of Defense, Bangaloru 560037, India

## 1 Introduction

The Doppler effect [1] comes into play when a signal is transmitted and received after being reflected by a moving target. Papic et al. [2, 3] estimated the Doppler shift through time-dependent Fourier analysis, using a rectangular window function. The rectangular window having an abrupt transition from and to zero outside the selected range is known to introduce ripples in the Fourier analysis. To alleviate the presence of large oscillations in both the pass band and the stop band, one should use a window function that ramps up and down towards zero gradually [4]. Hence the Kaiser window can be used in place of a rectangular window to obtain the finite sequence [5].

In [2], three consecutive peaks obtained from the spectrum were considered to minimize the error introduced by the estimated frequency. The optimized frequency was obtained using a simple interpolation procedure based on second-order polynomial approximation. Valarmathi et al. [6] considered three consecutive peaks of the finite sequence obtained with a Kaiser window [4], and used Lagrange's polynomial interpolation and semi-Newtonian iteration to determine the Doppler shift. Simulations showed that the above methods did not offer much improvement in the estimation. In these methods, the look-up table [2] was directly used to adapt the window length. In [7], target position and velocity are estimated via polynomial optimization using $n$-Doppler shift measurements collected at $n$ nodes in a sensor network. Similarly in [8], estimated velocity through FFT, was refined by the Hough detector in which the Hough parameter space is sampled incrementally to meet the needed accuracy requirements. These methods had much computational complexity.

The look-up table provides a window length for different signal-to-noise ratios (SNRs) at three constant accelerations, namely 3, 7 and 15 m/s$^2$. Other accelerations have to be approximated to these values in selecting the window length. This approximation results in errors in estimation.

The works of Papic et al. [2, 3], Katkovnik et al. [9], Jubisa et al. [10] and Hedrick [11] emphasize the importance of the length of the window function. Using a short-length window function helps avoid the effect of velocity averaging across a long interval but can result in poor velocity estimation and higher acceleration in the case of intensive object dynamics. In the case of a low SNR, a sufficient window length is crucial to obtain relevant information on the Doppler frequency shift. The trade-off between the echo signal's SNR and target acceleration is done carefully to determine the window length. It was observed that the method of interpolation was more effective in adapting the window length to determine acceleration. Furthermore, it was observed that interpolated Doppler filter with fast Fourier transformation gave a better estimate of velocity than the complicated methods described earlier. A Kalman filter [12, 13] was used to smooth the estimated velocity and determine the acceleration of the moving target.

This paper is organized as follows. The system description, Doppler frequency estimation and interpolation methods are explained in section 2. The Kalman filter structure and the window length adaptation are explained

in sections 3 and 4. In section 5, results of velocity estimation obtained with the algorithms described in previous sections are simulated and analyzed. Finally, the conclusion is given in section 6.

# 2 System description

A block diagram depicting velocity estimation is shown in Fig. 1. A Doppler filter is used to determine the Doppler shift from the echo signal. A sinusoidal signal transmitted by the radar antenna has the form $x_T(t) = A\cos\omega_0 t$, where $\omega_0$ is the angular frequency. This signal when reflected back from a stationary target results in a round-trip time delay $\tau = 2R/c$, where $R$ is the range of the target in kilometers and $c = 3\times10^8$ m/s is the velocity of light. The received signal is of the form

$$x_R(t) = A\cos\Omega_0(t-\tau). \tag{1}$$

In the case of a moving target, the received signal also has a phase difference (used to determine the velocity of the signal). The phase difference can be represented in terms of angular frequency $\Omega_d$ and is given by

$$\Omega_d = \frac{-2\Omega_0\frac{dR(t)}{dt}}{c}. \tag{2}$$

Hence, the received signal is of the form

$$x_R(t) = A\cos((\Omega_0-\Omega_d)t-\Omega_0\tau). \tag{3}$$

In a practical scenario, owing to the presence of noise, the received signal is assumed to be of the form

$$x_R(t) = A\cos((\Omega_0-\Omega_d)t-\Omega_0\tau)+v(t), \tag{4}$$

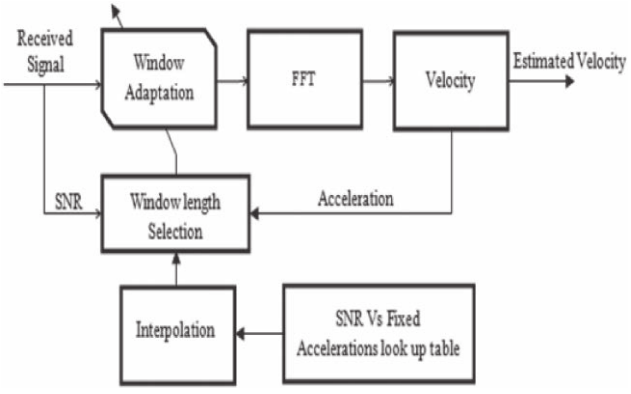


**Fig. 1:** Block diagram of velocity estimation

where $v(t)$ is random noise, which is statistically independent.

## 2.1 Windowing

In the case of a Kaiser window [1], there is the flexibility of choosing a desired side lobe level and main lobe peak by varying the parameter $\alpha$. An added advantage of the Kaiser window is that its transition bandwidth is always small. Here the stop band attenuation ($A_s$) is assumed to be 25 dB. Hence, $\beta = 0.6$ approximately.

## 2.2 Fast Fourier Transform (FFT)

The windowed output is analyzed in the frequency domain by performing the FFT to obtain the peak frequency:

$$X(k)\sum_{n=0}^{N-1}x(n)e^{-j2\pi nk/N};\quad 0\le k\le N-1. \tag{5}$$

A higher point FFT is applied to the window output so as to obtain a better display of the DFT $X(k)$. As the window size $M$ is less than $N$, zeros are used for padding. The frequency corresponding to the highest magnitude of the FFT is the received signal frequency $f_1$.

## 2.3 Velocity estimation

The Doppler frequency shift $f_d$ is given as the frequency by which the received signal varies from the transmitted signal. Hence, $\pm f_d = f_1 - f_0$, where $f_0$ is the transmitted-signal frequency. The velocity of the target is given by

$$v_p = f_d\times\frac{c}{f_0}\cos\theta, \tag{6}$$

where $\cos\theta = \cos\theta_a\cos\theta_e$; angles $\theta_e$ and $\theta_a$ are respectively the elevation and azimuth angles. For the estimated Doppler frequency shift, the target radial velocity $v_r$ can be calculated as

$$v_r = \frac{f_d c}{2f_0}. \tag{7}$$

## 2.4 Lagrangian interpolation technique

Since there are $N$ samples of the received signal, a proper sampling size should be selected through Kaiser window-

ing in the trade-off between determining the target maneuvering and the SNR. For each observation, the window length has to be adjusted according to the target acceleration and SNR. The look-up table [2] provides the window length for different SNRs at three constant accelerations, namely 3, 7 and 15 m/s$^2$. Other accelerations are approximated to these values in selecting the window length. This approximation leads to errors in estimation. Hence, the interpolation technique was used for the acceleration to adapt a better window length.

Using Lagrangian polynomials [14, 15, 16], it is possible to obtain the second-order interpolating polynomial $Q(f)$, which passes through three points $(f_1, X_1)$, $(f_2, X_2)$ and $(f_3, X_3)$ of the window length corresponding to the given accelerations:

$$Q(f) = L_1(f)X_1 + L_2(f)X_2 + L_3(f)X_3, \tag{8}$$

where $L_1(f)$, $L_2(f)$ and $L_3(f)$ are the Lagrangian polynomials given by

$$L_1(f) = \frac{(f - f_k)(f - f_{k+1})}{(f_{k-1} - f_k)(f_{k-1} - f_{k+1})},$$
$$L_2(f) = \frac{(f - f_{k-1})(f - f_{k+1})}{(f_k - f_{k-1})(f_k - f_{k+1})},$$
$$L_3(f) = \frac{(f - f_k)(f - f_{k-1})}{(f_{k+1} - f_k)(f_{k+1} - f_{k-1})}.$$

The frequency $f$ is the approximate solution of the polynomial $Q(f)$. It is noted that the velocity estimated using the interpolated adaptive Doppler filter with only the FFT is better than that estimated using the complicated methods mentioned earlier. However, the initial estimation still contains more error.

## 2.5 Cubic spline interpolation

To reduce the error in the initial estimation [15], instead of Lagrangian interpolation, the cubic spline method was used. Cubic splines are curves used for the interpolation of data. They are constructed through a set of known data points. Here, corresponding to the SNR of the received signal, the accelerations and the respective window lengths obtained from the look-up table given in [2] are interpolated through cubic spline interpolation. In cubic spline interpolation, there are generally equations for two splines [14, 16]:

$$y = a_1(x - x_1)^3 + b_1(x - x_1)^2 + c_1(x - x_1) + d_1, \tag{9}$$

$$y = a_2(x - x_2)^3 + b_2(x - x_2)^2 + c_2(x - x_2) + d_2, \tag{10}$$

where $x$ is acceleration and $y$ is the window length, and $a_1$, $a_2$, $b_1$, $b_2$, $c_1$, and $c_2$ and $d_1$ and $d_2$ are constants. Substituting $x = x_1$ and $x = x_2$ into equations (9) and (10) gives

$$d_1 = y_1 \quad \text{and} \quad d_2 = y_2.$$

Taking the second derivative of equations (9) and (10) yields

$$y'' = 6a_1(x - x_1) + 2b_1, \tag{11}$$

$$y'' = 6a_2(x - x_2) + 2b_2. \tag{12}$$

Considering that $y'' = y_1''$ at $x = x_1$ in equation (11) and $y'' = y_2''$ at $x = x_2$ in equation (12), we have

$$b_1 = y_1''/2 \quad \text{and} \quad b_2 = y_2''/2. \tag{13}$$

Substituting equation (13) into equations (11) and (12) and solving the same after letting $y'' = y_1''$ at $x = x_1$ in equation (11) and $y'' = y_2''$ at $x = x_2$ in equation (12), we have

$$a_1 = (y_2'' - y_1'')/6h_1; \quad a_2 = (y_3'' - y_2'')/6h_2, \tag{13}$$

where $h_1 = x_2 - x_1$ and $h_2 = x_3 - x_2$.

Substituting all the constants and setting $y = y_1$ at $x = x_1$ and $y = y_2$ at $x = x_2$ in equations (9) and (10), we have

$$\begin{aligned} c_1 &= (y_2 - y_1)/h_1 - y_2''h_1/6 - y_1''h_1/3, \\ c_2 &= (y_3 - y_2)/h_2 - y_3''h_2/6 - y_2''h_2/3. \end{aligned} \tag{14}$$

Finally, to find the unknown second derivatives, we impose the compatibility condition that $y_2'$ in spline 1 must equal $y_2'$ in spline 2:

$$\begin{aligned} 3a_1(x_2 - x_1)^2 + 2b_1(x_2 - x_1) + c_1 = 3a_2(x_2 - x_2)^2 \\ + 2b_2(x_2 - x_2) + c_2. \end{aligned} \tag{15}$$

The substitution of all constants in equation (15) and subsequent simplification lead to

$$\begin{aligned} h_1y_1'' + 2(h_1 + h_2)y_2'' + h_2y_3'' \\ = 6[(y_3 - y_2)/h_2 - (y_2 - y_1)/h_1]. \end{aligned} \tag{16}$$

If we consider the natural boundary conditions $y_1'' = 0$ and $y_3'' = 0$ in equation (16), we have the matrix equation

$$y_2'' = \frac{6[(y_3 - y_2)/h_2 - (y_2 - y_1)/h_1]}{2(h_1 + h_2)}. \tag{17}$$

The given window lengths corresponding to the three acceleration values are taken as $(x_1, y_1)$, $(x_2, y_2)$ and $(x_3, y_3)$,

and the spline segment coefficients are calculated and the cubic spline is plotted. From the cubic spline plotted, the exact window length is obtained for a particular acceleration pertaining to a particular SNR.

# 3 Kalman filter

Here the Kalman filter is used to smooth the noisy measurement obtained with the Doppler filter. The inputs of the Kalman filter are the velocity estimates obtained with the Doppler filter and the outputs are the refined velocity estimates. The state space representation of object kinematics is given by

$$\boldsymbol{Z}(\boldsymbol{k}) = \phi(\boldsymbol{k})\boldsymbol{Z}(\boldsymbol{k-1}) + \omega(k), \tag{18}$$

where $\boldsymbol{Z}(\boldsymbol{k})$ is the state vector $[v(k) \quad a(k)]'$, and $v(k)$ and $a(k)$ are the velocity and acceleration of the target respectively. $\phi(k)$ is the state transition matrix $\begin{vmatrix} 1 & T \\ 0 & 1 \end{vmatrix}$. We assume the measurement equation has the algebraic form

$$\boldsymbol{Y}(\boldsymbol{k}) = \boldsymbol{H}\boldsymbol{Z}(\boldsymbol{k}) + \mu(k), \quad \text{where } \boldsymbol{H} = [1 \quad 0]. \tag{19}$$

The random variables $\omega(k)$ and $\mu(k)$ represent the process and measurement noise, which are white Gaussian noise with covariance matrices $Q(k)$ and $R(k)$ respectively. The Kalman filter estimates a state at some point in time and then obtains feedback in the form of a noisy measurement. These two steps are called prediction and correction [12, 13].

## 3.1 Prediction

$$\begin{aligned} \hat{\boldsymbol{Z}}\left(\frac{\boldsymbol{k}}{\boldsymbol{k-1}}\right) &= \phi(\boldsymbol{k})\hat{\boldsymbol{Z}}\left(\frac{\boldsymbol{k-1}}{\boldsymbol{k-1}}\right) \\ \boldsymbol{P}\left(\frac{\boldsymbol{k}}{\boldsymbol{k-1}}\right) &= \phi(\boldsymbol{k})\boldsymbol{P}\left(\frac{\boldsymbol{k-1}}{\boldsymbol{k-1}}\right)\phi(\boldsymbol{k})' + Q(k) \end{aligned} \tag{20}$$

## 3.2 Correction

$$K(k) = \boldsymbol{P}\left(\frac{\boldsymbol{k}}{\boldsymbol{k-1}}\right)\boldsymbol{H}^{\boldsymbol{T}}\left[\boldsymbol{H}\boldsymbol{P}\left(\frac{\boldsymbol{k}}{\boldsymbol{k-1}}\right)\boldsymbol{H}^{\boldsymbol{T}}\boldsymbol{R}(\boldsymbol{k})\right]^{-1} \tag{21}$$

$$\hat{\boldsymbol{Z}}\left(\frac{\boldsymbol{k}}{\boldsymbol{k}}\right) = \hat{\boldsymbol{Z}}\left(\frac{\boldsymbol{k}}{\boldsymbol{k-1}}\right) + K(k)[\boldsymbol{Y}(\boldsymbol{k}) - \boldsymbol{H}\boldsymbol{Z}\boldsymbol{k}\boldsymbol{k-1}] \tag{22}$$

$$\boldsymbol{P}\left(\frac{\boldsymbol{k}}{\boldsymbol{k}}\right) = \boldsymbol{P}\left(\frac{\boldsymbol{k}}{\boldsymbol{k-1}}\right) - K(k)\boldsymbol{H}\boldsymbol{P}\left(\frac{\boldsymbol{k}}{\boldsymbol{k-1}}\right) \tag{23}$$

Here $\boldsymbol{P}\left(\frac{\boldsymbol{k}}{\boldsymbol{k-1}}\right)$ and $\boldsymbol{P}\left(\frac{\boldsymbol{k}}{\boldsymbol{k}}\right)$ are the prediction and correction errors. The first task during the correction step is to compute the Kalman filter gain $K(k)$ according to equation (21). The next step is to generate an *a posteriori* state estimate $\hat{\boldsymbol{Z}}\left(\frac{\boldsymbol{k}}{\boldsymbol{k}}\right)$ whose elements are the unknown target velocity and acceleration, by incorporating the measurement as in equation (22). The final step is to obtain an *a posteriori* error covariance estimate via equation (23).

# 4 Adaptive Kalman filter

The target may undergo different accelerations. As a result, frequency also changes with time. Since we are considering a fixed window length in Doppler and Kalman filters, there is a delay in tracking the target dynamics [1, 2, 12]. The applied window function length must be short enough to avoid the effect of velocity averaging over a long interval. This velocity averaging would result in poor velocity estimation in the case of intensive object dynamics resulting in greater acceleration. On the other hand, the window length has to be long enough to contain relevant information on the Doppler frequency shift especially in the case of a low SNR. This is in accordance with the known results in the literature [2, 3, 11]. Therefore, in adaptive Kalman filtering, a proper window length is chosen according to the acceleration of the target and SNR. Using the Kalman filter, the target velocity and acceleration are estimated. The next unknown is the SNR, which can be estimated as follows.

Proper window lengths for different accelerations with the SNR as a parameter are presented in reference [2]. On the basis of the received-signal SNR and the acceleration estimated with the Kalman filter, if we select the window length particularly at a low SNR, the estimated frequency has more error as shown in the simulation result. Hence, cubic spline interpolation is used to select the proper window length from the interpolated accelerations [2]. Spline interpolation equations are given in equations (5) to (12). Here the inputs are the known window length for the estimated accelerations.

## 4.1 Choice of optimal window length

The window length that has less cumulative estimation error (cee) is taken as the optimal length. Thus, cee is given as

$$cee(k) = \frac{1}{k}\sum_{j=1}^{k}\frac{|v(j)-\hat{v}(j)|}{|v(j)|}. \quad (24)$$

Cumulative error is estimated (*cee*) for the set of estimated velocities with different window lengths for the estimated SNR.

### 4.2 SNR estimation

$$\hat{SNR} = 10\log\frac{\hat{A}^2}{\hat{\sigma}_{\mu}^2(k)}, \quad (25)$$

where $\hat{A}^2$ is the estimated signal amplitude,

$$\hat{\sigma}_{\mu}^2(k) = \hat{d}^2(k) - \boldsymbol{HP}\left(\frac{\boldsymbol{k}}{\boldsymbol{k}}\right)\boldsymbol{H}^{\boldsymbol{T}},$$
$$\hat{d}(k) = median\frac{|\hat{\mu}(k) - median(\mu(k))|}{0.6745}, \quad (26)$$

$$\hat{\boldsymbol{\mu}}(\boldsymbol{k}) = \boldsymbol{Y}(\boldsymbol{k}) - \boldsymbol{H}\hat{\boldsymbol{Z}}\left(\frac{\boldsymbol{k}}{\boldsymbol{k}}\right) \quad (27)$$

## 5 Results and analyses

Here it is assumed that data are received by a radar system every 2 ms. The maximum number of samples for processing is 5000; i.e., the period of observation is $5000 \times 2 \times 10^{-3} = 10$ s. With fast maneuvering of the target, the target velocity is assumed to change from 250 to 116.6 m/s within 3.6 s. This gives the acceleration as 37.13 m/s$^2$. Figures 2 and 3 show the Lagrange and spline-interpolated window lengths, corresponding to the interpolated accelerations at different SNRs according to reference [2].

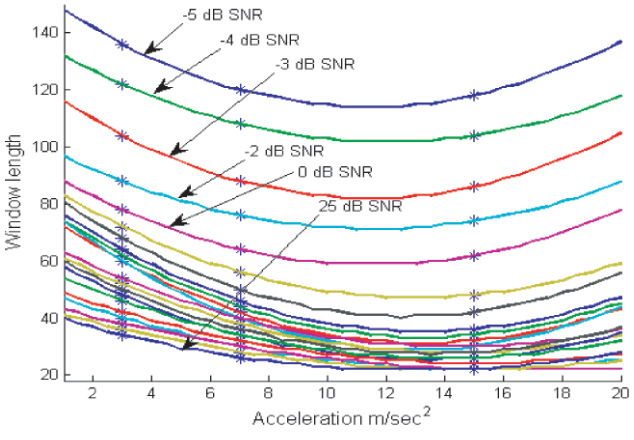


**Fig. 2:** Lagrange's interpolated acceleration versus window length for different SNRs

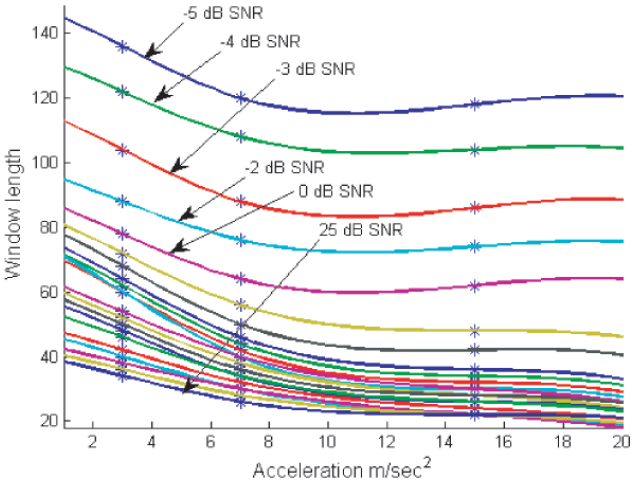


**Fig. 3:** Spline-interpolated acceleration versus window length for different SNRs

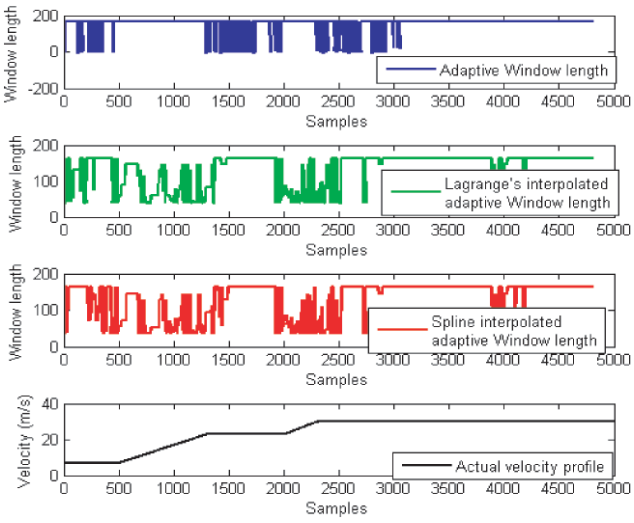


**Fig. 4:** Window length adaptation without and with interpolation for path 1 at a SNR of 5 dB

Figures 4 and 8 show the window length adaptation without and with interpolation for the velocity profile with acceleration of path 1 at 5 dB and an SNR of 25 dB. It is seen that the velocity estimation is better with the interpolated adaptive window length as shown in Figs. 6 and 7 compared with Fig. 5. Velocity is better estimated employing Kalman smoothing. The same analyses are made at an SNR of 25 dB as shown in Figs. 9 to 11. It is seen that the velocity is well estimated with the combination of the interpolated adaptive Doppler filter and Kalman smoothing at a low SNR. Even though the window length adaptation seems the same with and without interpolation as seen in

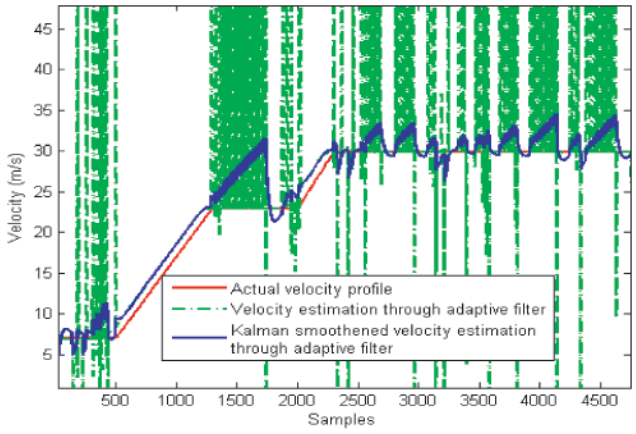


**Fig. 5:** Velocity estimation with an adaptive window length for path 1 at a SNR of 5 dB

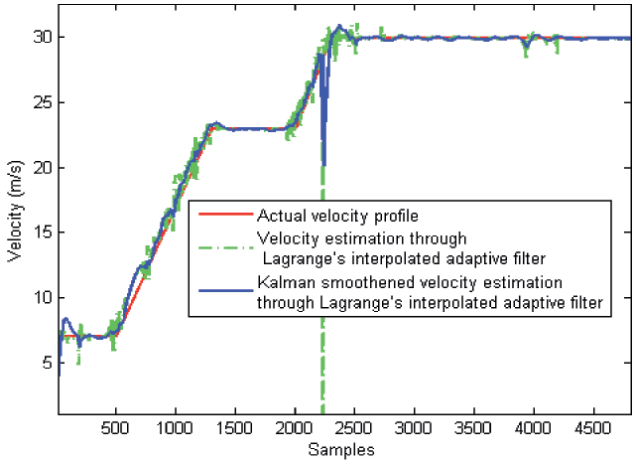


**Fig. 6:** Velocity estimation with a Lagrange-interpolated adaptive window length for path 1 at a SNR of 5 dB

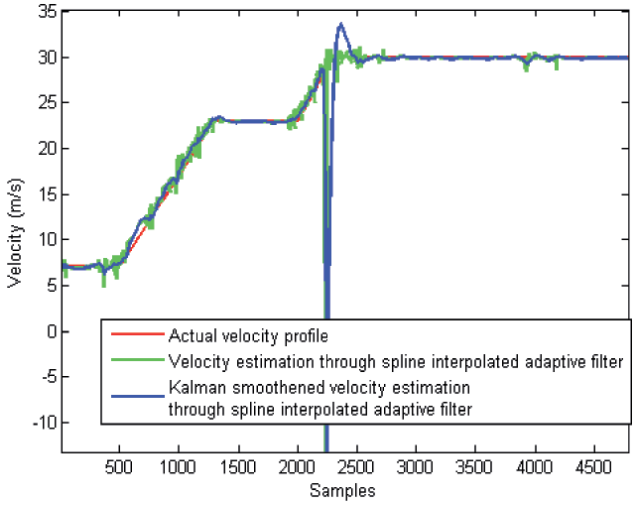


**Fig. 7:** Velocity estimation with a spline-interpolated adaptive window length for path 1 at a SNR of 5 dB

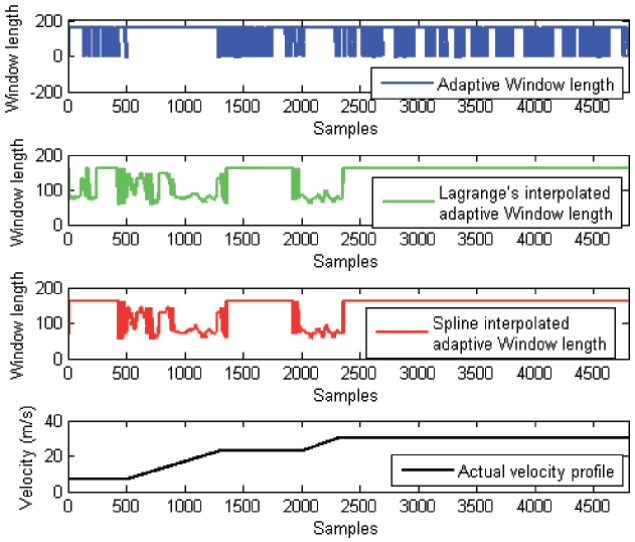


**Fig. 8:** Window length adaptation without and with interpolation for path 1 at a SNR of 25 dB

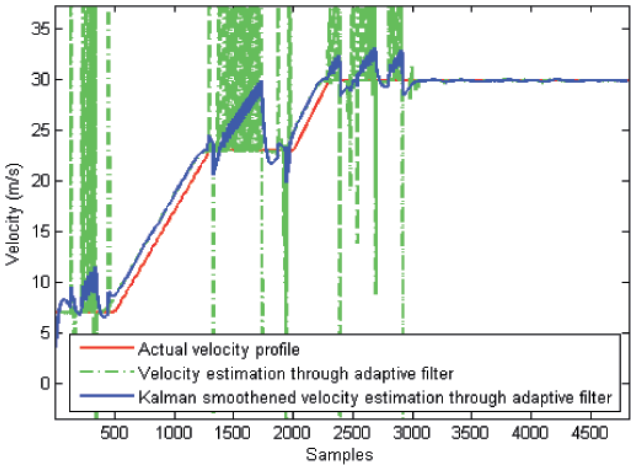


**Fig. 9:** Velocity estimation with an adaptive window length for path 1 at a SNR of 25 dB

Figures 4 and 8, the performance of the velocity estimation is markedly improved with interpolation as shown in Figs. 9 and 10.

Figures 12 and 16 show the adaptive window length without and with interpolation for the velocity profile with deceleration of path 2 at 5 dB and an SNR of 25 dB. It is observed that estimated velocity obtained through interpolated adaptive Doppler filter is better in this path 2 (as shown in Figures 14, 15, 18 and 19) than the algorithms mentioned earlier shown in Figures 13 and 17. Error in the track initialization is reduced in the spline interpolated method compared to the Lagrangian interpolation.

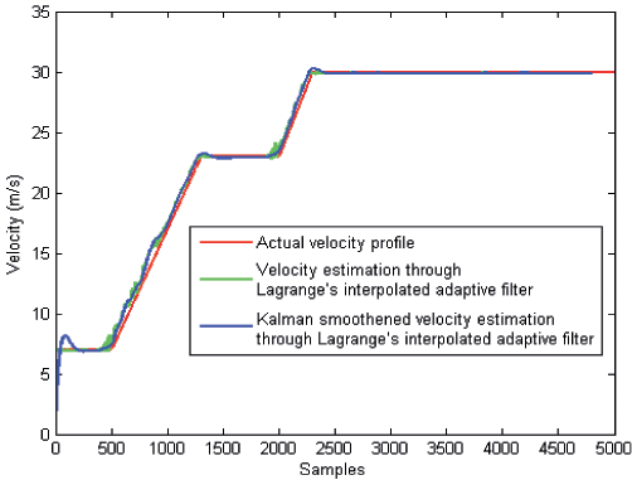


**Fig. 10:** Velocity estimation with a Lagrange-interpolated adaptive window length for path 1 at a SNR of 5 dB

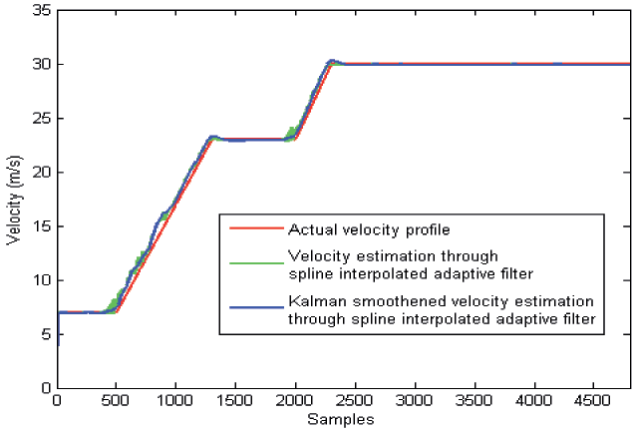


**Fig. 11:** Velocity estimation with a spline-interpolated adaptive window length for path 1 at a SNR of 25 dB

Cumulative error estimation (cee) plots are shown in Figs. 20 to 23 for paths 1 and 2 at 5 dB and an SNR of 25 dB. In all plots, it is observed that *cee* is lower in the velocity estimation made with the interpolated adaptive Doppler filter than in the case for the adaptive filter.

## 6 Conclusion

The results of this study clearly show that interpolated window length adaptation provides better velocity estimation than the previously employed method of estimating the Doppler shift through time-dependent Fourier analysis using a rectangular window function. In general, track initialization is a challenging task, mostly accepted with an allowable error. It was observed that this error is reduced with spline interpolation compared with Lagrange interpolation. Additionally, velocity estimation

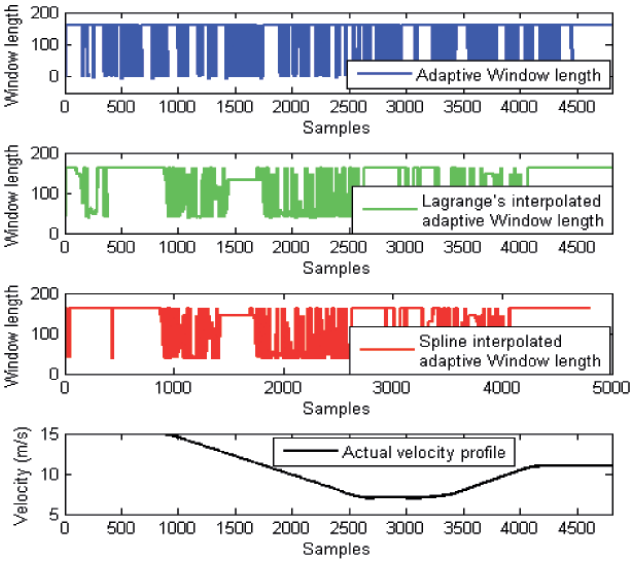


**Fig. 12:** Window length adaptation without and with interpolation for path 2 at a SNR of 5 dB

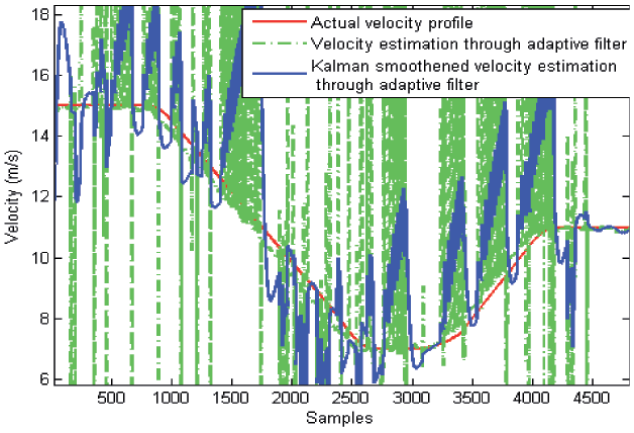


**Fig. 13:** Velocity estimation with an adaptive window length for path 2 at a SNR of 5 dB

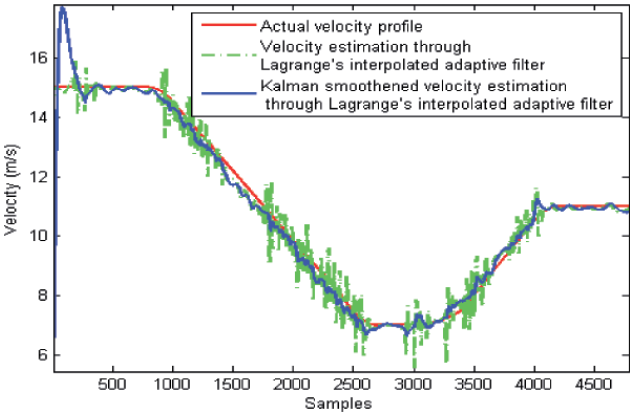


**Fig. 14:** Velocity estimation with a Lagrange-interpolated adaptive window length for path 2 at a SNR of 5 dB

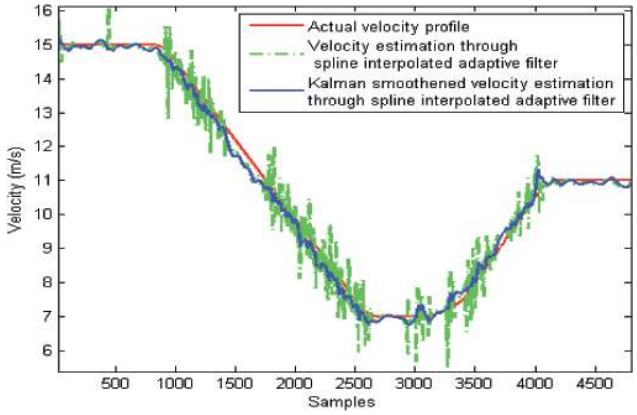


**Fig. 15:** Velocity estimation with a spline-interpolated adaptive window length for path 2 at a SNR of 5 dB

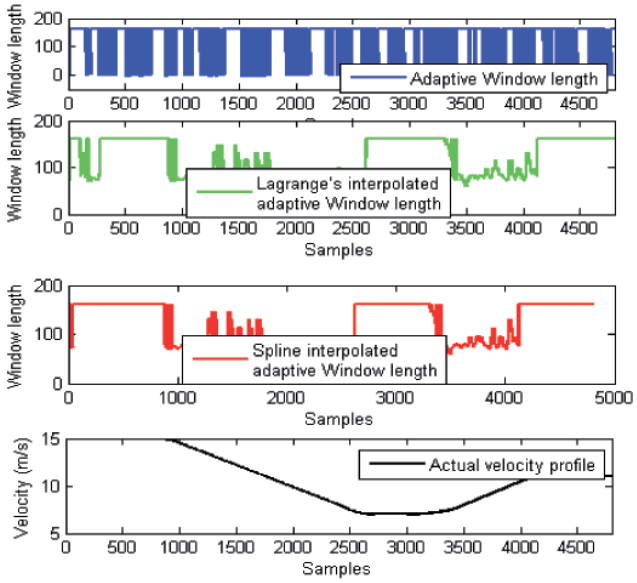


**Fig. 16:** Window length adaptation without and with interpolation for path 2 at a SNR of 25 dB

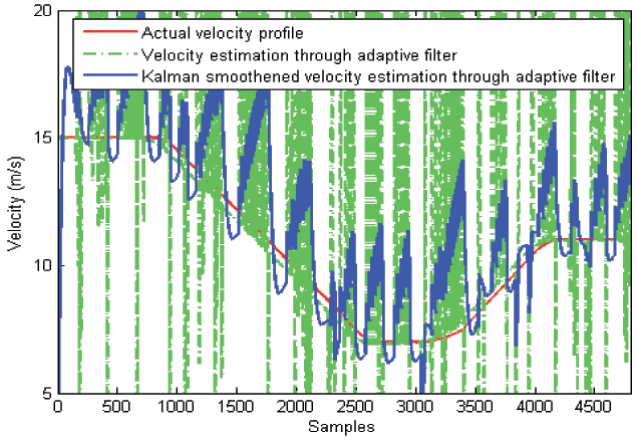


**Fig. 17:** Velocity estimation with an adaptive window length for path 2 at a SNR of 25 dB

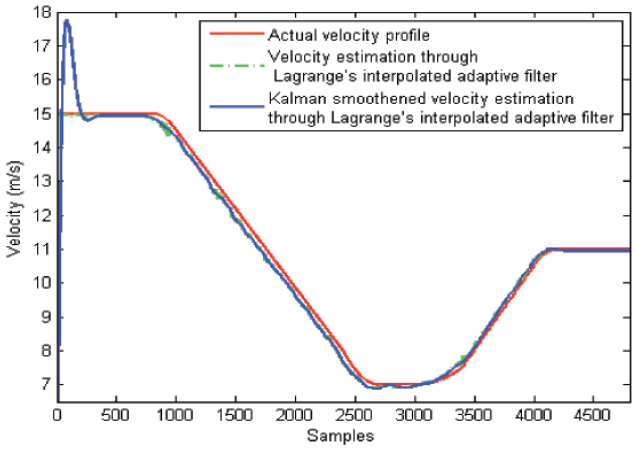


**Fig. 18:** Velocity estimation with a Lagrange-interpolated adaptive window length for path 2 at a SNR of 25 dB

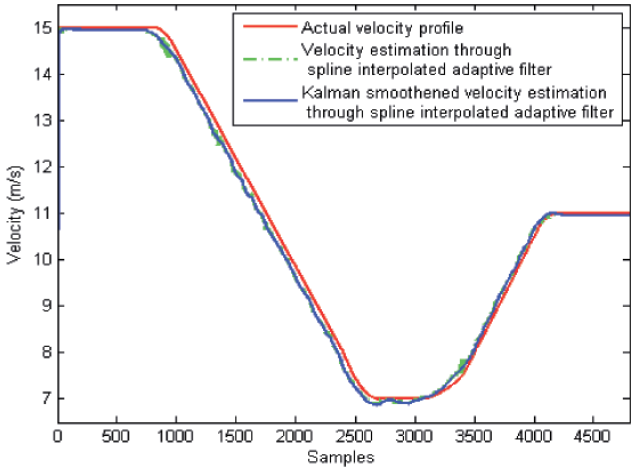


**Fig. 19:** Velocity estimation with a spline-interpolated adaptive window length for path 2 at a SNR of 25 dB

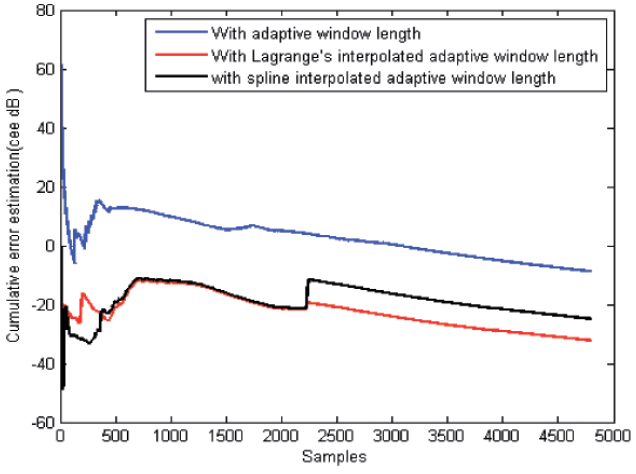


**Fig. 20:** Cumulative error analysis for path 1 at 5 dB SNR

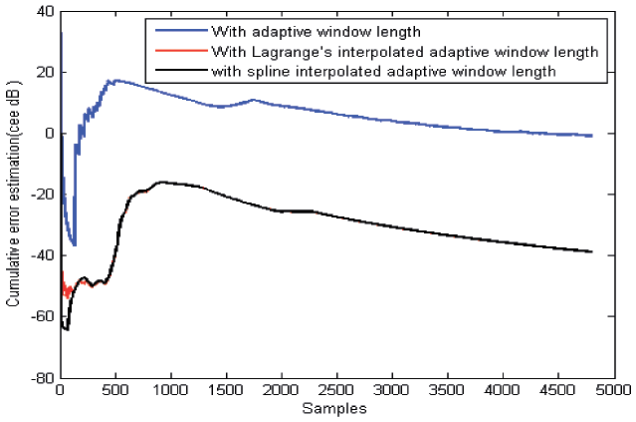


**Fig. 21:** Cumulative error analysis for path 1 at a SNR of 25 dB

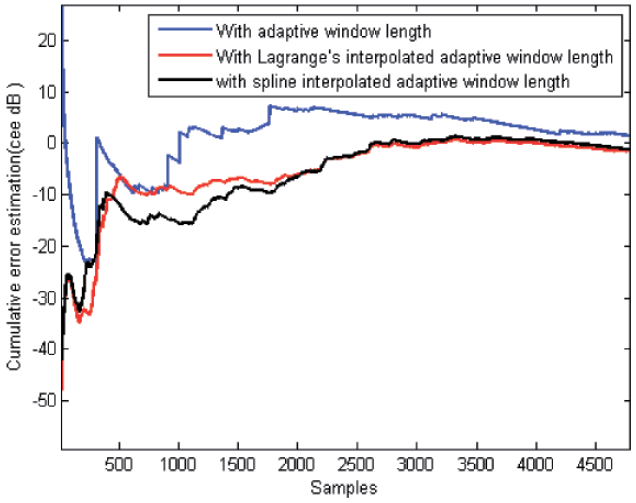


**Fig. 22:** Cumulative error analysis for path 2 at a SNR of 5 dB

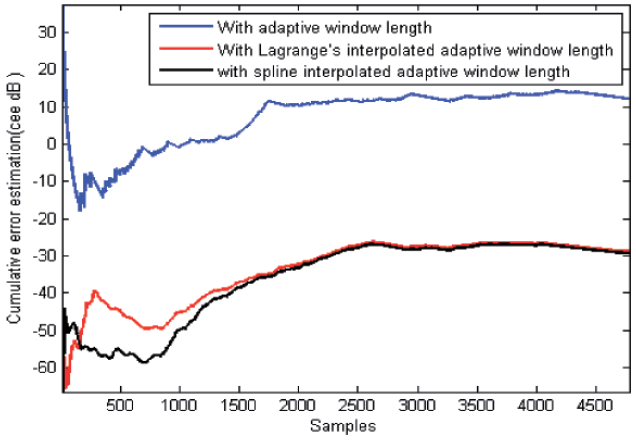


**Fig. 23:** Cumulative error analysis for path 2 at a SNR of 25 dB

improved when the target was accelerating rather than decelerating. Fighter aircraft with velocity of 1.7 mach and accelerations of 9 to –3.5 g (88.2 to –34.3 m/s$^2$) may be reliably tracked using our algorithm. Other interpolation techniques can also be used to compare the efficiency of the window length.

Received: October 28, 2012.

## References

[1] Skolnik MI (1976). Radar Systems. McGraw-Hill, New York, 2001.
[2] Papic VD, Djurovic ZM, Kovacevic BD (2006). Adaptive Doppler–Kalman filter for radar systems. IEE Proc–Vis Image Signal Process 153(3): 379–387.
[3] Papic VD, Djurovic ZM, Kovacevic BD (2002). Adaptive Doppler filters using simultaneous estimation of target acceleration and signal to noise ratio. 10th Telecommunications Forum, Belgrade, Yugoslavia, Nov. 2002, 26–28.
[4] Oppenheim AV, Schafer RW (1999). Discrete-time signal processing, 2nd edition. Prentice-Hall, New Jersey.
[5] Verma T, Bilbao S, Meng THY (1996). The digital prolate spheroidal window. IEEE International Conference on Acoustics, Speech, and Signal Processing 3:1351–1354.
[6] Valarmathi J, Emmanuel DS, Christopher S (2011). Doppler information optimization through fusion algorithms. International Journal of Computer Applications 27(11):37–43.
[7] Shames I, Bishop AN, Smith M, Anderson BDO (2013). Doppler Shift Target Localization. IEEE Transactions on Aerospace and Electronic Systems, Volume 49, Issue 1, pp. 266–276.
[8] Doukovska L (2011). Alternative approaches for target velocity estimation using the Hough transform in MIMO radar systems. Cybernetics and Information Technologies, Volume 11, No. 1, pp. 45–63.
[9] Katkovnik V, Stankovic LJ (1998). Instantaneous frequency estimation using Wigner distribution with varying and data driven window length. IEEE Transactions on Signal Processing 46(9), 2315–2325.
[10] Jubisa Stankovic L, Katkovnik V (1998). Algorithm for the instantaneous frequency estimation using time frequency distributions with adaptive window width. IEEE signal Processing Letters 5(9), 224–227.
[11] Hedrick JK, Jang J, Potier A (2004). Cooperative multiple-sensor fusion for automated vehicle control. Research report, University of California, Berkeley.
[12] Schmidt SF (1981). The Kalman filter, its recognition and development for aerospace applications. AIAA J Guidance Control 4(1):4–7.
[13] Kalman RE (1960). A new approach to linear filtering and prediction problems. Trans ASME, Set D, J Basic Eng 82:35–45.
[14] Griffiths DV, Smith IM (1991). Numerical methods for engineers. CRC Press, Great Britain.
[15] Valarmathi J, Emmanuel DS, Christopher S (2012). Velocity Tracking Based on Interpolated Adaptive Doppler Filter. Fusion'12 conference, 9th–12th July 2012, Singapore.
[16] Butt R (2008). Introduction to Numerical Analysis using MATLAB. Boston Infinity Science Press LLC, Boston.